

Minimum Thickness for Ice Dome Subjected to a Human Live Load

Tsutomu Kokawa

School of Art and Technology, Hokkaido Tokai University
Asahikawa, Hokkaido, Japan

ABSTRACT

This paper describes a numerical investigation of structural safety where the ice dome is subjected to a concentrated load such as a human live load on the apex. Regarding the problem as a short-term loading and the elastic behavior of ice, the elastic solution is based on the theory of a spherical shallow shell under a small circular uniform load. The cases of both single and twin loads on a dome are investigated, assuming that the ice dome will break when the tensile stress reaches a certain maximum value. Estimating that the weight of a human is 100 kg and the allowable stress of the ice is 3 kg/cm^2 , where the flexural strength is 10 kg/cm^2 , it is concluded that the minimum thickness for the ice is 6 cm for spans up to 15 m, and 7 cm for spans between 15 m and 30 m. It is also true for twin loads when the loading distance is 1 m apart.

KEY WORDS: Ice Dome, Human live load, Short-term structural safety, Small circular uniform load, Minimum ice thickness

INTRODUCTION

Ice shells are being used as winter architectural structures in inland Hokkaido, where the volume of snow and sustained sub-freezing temperatures make conditions favorable (Kokawa *et al.*, 2000). The ice shell creates a beautiful space in the environment from the translucent thin plate and the unique curved surface form. The interior space has a lunescence atmosphere with full of natural light in daytime, and the exterior looks like a gigantic chandelier in the dark at night. As the typical example of the applications, since 1997 in Tomamu, many ice shells are being used each winter for about 3 months as leisure-recreational facilities as shown in Fig.1. The construction method of blowing snow and spraying water onto an pneumatic formwork has constructional rationality (Kokawa, 1985), having taken only one week to complete ice domes spanning 20 to 30 meters in the past field experiments (Kokawa, 2002). The shell has also high structural efficiency, because the form determined from the reticular geometry of the covered ropes in the formwork follows automatically so that the



Fig.1 Ice Shells in Tomamu (2002-2003 winter)



Fig.2 Spraying water on ice dome under construction

membrane stresses are mainly compressive under self-weight load. The experimental studies on the structural engineering problems (Kokawa and Murakami, 1986; Kokawa, 1988) and the practical applications in ice shell construction have been conducted in the winter environment of Hokkaido since 1980s. As the result, it is recognized that the ice shell is a practical ice structure for winter activities in snowy and cold regions. However, there are still engineering problems to be solved concerning design, construction, structural safety and maintenance in order to realize a reliable structure. The greatest importance are the problems concerning structural safety.

This paper describes a numerical investigation of minimum thickness for ice dome under short-term concentrated loading. Workers occasionally go up on the ice dome under various situations such as snow removal and the water spraying in the construction process as shown in Fig.2. In such situation, the minimum thickness of the ice should be determined to ensure safety. A local bending stress occurs at the vicinity of the concentrated loading point and may cause a fatal fracture in the case of a brittle material such as ice. Therefore the structural safety of the ice dome must be investigated when the ice dome is subjected to a concentrated load such as a human live load on the apex. Regarding the problem as a short-term loading and the elastic behavior of ice, the elastic solution is based on the theory of a spherical shallow shell under a small circular uniform load. The cases of both single and twin loads on a dome are numerically investigated, assuming that the ice dome will break when the tensile stress reaches a certain maximum value.

ELASTIC SOLUTION OF CIRCULAR UNIFORM LOAD

Solution of Vertical Displacement and Stress Function

The differential equations are given in Eq.(1) where a shallow spherical shell is subjected to a uniformly circular load, as shown in Fig.3 (Timoshenko,S. P. and Woinoesky-Krieger,S., 1959a).

$$\text{Equilibrium equation: } \Delta\Delta w - \frac{1}{DR} \Delta F = \frac{qG(r, a)}{D} \quad \left. \right\} \quad (1)$$

$$\text{Compatibility equation: } \Delta\Delta F + \frac{Eh}{R} \Delta w = 0$$

Where $\Delta = \frac{d^2}{dr^2} + \frac{1}{r} \frac{d}{dr}$, w is the vertical displacement, F is the stress function, R is the radius of curvature of the shell,

$D \left(= \frac{Eh^3}{12(1-\nu^2)} \right)$ is flexural rigidity of the plate, h is the shell thickness, E

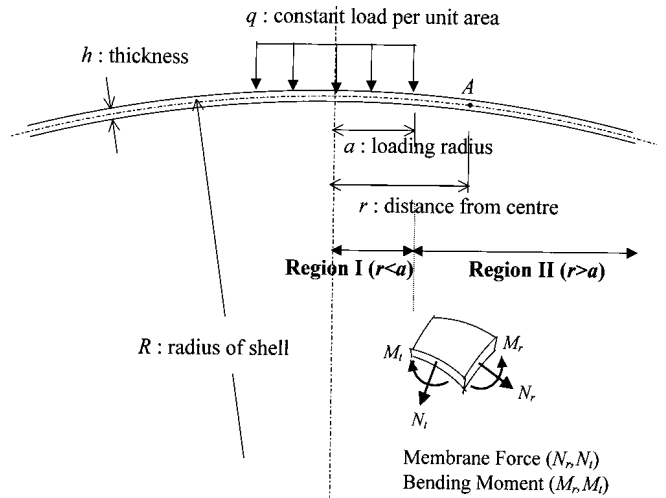


Fig.3 Spherical shallow shell under uniformly circular load

is Young's modulus, ν is Poisson's ratio and q is the constant load per unit area over the circle with radius a . Function G is as follows:

$$G(r, a) = \begin{cases} 1, & 0 \leq r \leq a \\ 0, & r \geq a \end{cases}$$

The solutions of w and F are given by the equations (2) and (3) for each region (see APPENDIX-1).

In the region I ($x < a$),

$$\left. \begin{aligned} w &= \frac{RP_t}{Eh^2} \frac{\sqrt{12(1-\nu^2)}}{\pi} \left(\left(\frac{\ker' \alpha}{\alpha} \right) berx - \left(\frac{kei' \alpha}{\alpha} \right) beix + \frac{1}{\alpha^2} \right) \\ F &= \frac{RP_t}{\pi} \left\{ \left(-\frac{kei' \alpha}{\alpha} \right) berx - \left(\frac{\ker' \alpha}{\alpha} \right) beix - \frac{1}{2} \log \alpha + \frac{1}{4} \left(1 - \left(\frac{x}{\alpha} \right)^2 \right) \right\} \end{aligned} \right\} \quad (2)$$

Where $P_t = \pi a^2 q$, P_t is the total load, $x = \frac{r}{l}$, $l^2 = \frac{Rh}{\sqrt{12(1-\nu^2)}}$, l is characteristic length, $\alpha = \frac{a}{l}$, \ker, bei, ber, kei and kei are Kelvin functions.

In the region II ($x > a$),

$$\left. \begin{aligned} w &= \frac{RP_t}{Eh^2} \frac{\sqrt{12(1-\nu^2)}}{\pi} \left\{ \left(\frac{ber' \alpha}{\alpha} \right) \ker x - \left(\frac{bei' \alpha}{\alpha} \right) kei x \right\} \\ F &= \frac{RP_t}{\pi} \left\{ \left(-\frac{bei' \alpha}{\alpha} \right) \ker x - \left(\frac{ber' \alpha}{\alpha} \right) kei x - \frac{1}{2} \log x \right\} \end{aligned} \right\} \quad (3)$$

Solution of Bending Moments and Membrane Forces

The relationship between the bending moments M_r and M_t , the membrane forces N_r and N_t , shown in Fig.3 and the displacement w , the stress function F , are expressed as follows:

$$\left. \begin{aligned} M_r &= -D\left(\frac{d^2w}{dr^2} + \frac{v}{r} \frac{dw}{dr}\right), & M_i &= -D\left(\frac{1}{r} \frac{dw}{dr} + v \frac{d^2w}{dr^2}\right) \\ N_r &= \frac{1}{r} \frac{dF}{dr}, & N_i &= \frac{d^2F}{dr^2} \end{aligned} \right\} \quad (4)$$

In the region I ($x < \alpha$),

Substituting Eq. (2) for Eq.(4), Eqs. (5) and (6) are given as follows:

$$M_{r1} = -\left(\frac{P_t}{\pi}\right) \left[\left(\frac{\ker' \alpha}{\alpha}\right) \left\{ -beix - (1-v) \frac{ber' x}{x} \right\} - \left(\frac{kei' \alpha}{\alpha}\right) \left\{ berx - (1-v) \frac{bei' x}{x} \right\} \right] \quad (5)$$

$$M_{i1} = -\left(\frac{P_t}{\pi}\right) \left[\left(\frac{\ker' \alpha}{\alpha}\right) \left\{ -vbeix + (1-v) \frac{ber' x}{x} \right\} - \left(\frac{kei' \alpha}{\alpha}\right) \left\{ vberx + (1-v) \frac{bei' x}{x} \right\} \right] \quad (5)$$

$$N_{r1} = -\left(\frac{P_t}{h}\right) \left(\frac{\sqrt{12(1-v^2)}}{\pi}\right) \left\{ \left(\frac{kei' \alpha}{\alpha}\right) \frac{ber' x}{x} + \left(\frac{\ker' \alpha}{\alpha}\right) \frac{bei' x}{x} + \frac{1}{2\alpha^2} \right\} \quad (6)$$

$$N_{i1} = -\left(\frac{P_t}{h}\right) \left(\frac{\sqrt{12(1-v^2)}}{\pi}\right) \left\{ \left(\frac{kei' \alpha}{\alpha}\right) \left(-beix - \frac{ber' x}{x}\right) + \left(\frac{\ker' \alpha}{\alpha}\right) \left(berx - \frac{bei' x}{x}\right) + \frac{1}{2\alpha^2} \right\} \quad (6)$$

In the region II ($x > \alpha$),

Substituting Eq. (3) for Eq.(4), Eqs. (7) and (8) are given as follows:

$$M_{rII} = -\left(\frac{P_t}{\pi}\right) \left[\left(\frac{ber' \alpha}{\alpha}\right) \left\{ -keix - (1-v) \frac{\ker' x}{x} \right\} - \left(\frac{bei' \alpha}{\alpha}\right) \left\{ kerx - (1-v) \frac{kei' x}{x} \right\} \right] \quad (7)$$

$$M_{iII} = -\left(\frac{P_t}{\pi}\right) \left[\left(\frac{ber' \alpha}{\alpha}\right) \left\{ -vkeix + (1-v) \frac{\ker' x}{x} \right\} - \left(\frac{bei' \alpha}{\alpha}\right) \left\{ vkerx + (1-v) \frac{kei' x}{x} \right\} \right] \quad (7)$$

$$N_{rII} = -\left(\frac{P_t}{h}\right) \left(\frac{\sqrt{12(1-v^2)}}{\pi}\right) \left\{ \left(\frac{bei' \alpha}{\alpha}\right) \frac{\ker' x}{x} + \left(\frac{ber' \alpha}{\alpha}\right) \frac{kei' x}{x} + \frac{1}{2x^2} \right\} \quad (8)$$

$$N_{iII} = -\left(\frac{P_t}{h}\right) \left(\frac{\sqrt{12(1-v^2)}}{\pi}\right) \left\{ \left(\frac{bei' \alpha}{\alpha}\right) \left(-keix - \frac{\ker' x}{x}\right) + \left(\frac{ber' \alpha}{\alpha}\right) \left(kerx - \frac{kei' x}{x}\right) - \frac{1}{2x^2} \right\} \quad (8)$$

NUMERICAL ANALYSIS

Single Load

A single uniformly circular load is discussed in this section. Here, the maximum tension stress σ_{max} occurs on the inner surface at the centre of the load and σ_{max} is given by Eq. (9) using Eqs.(5) and (6).

$$\sigma_{\text{max}} = \left[\left(\frac{M_{r1}}{\left(\frac{h^2}{6}\right)} + \frac{N_{r1}}{h} \right) \right]_{x=0} = \frac{1}{k_s} \left(\frac{P_t}{h^2} \right) \quad (9)$$

where, k_s is loading coefficient.

$$k_s = \frac{1}{\left(\frac{3}{\pi}\right)(1+v) \left(\frac{kei' \alpha}{\alpha}\right) - \left(\frac{\sqrt{3(1-v^2)}}{\pi}\right) \left(\frac{\ker' \alpha}{\alpha} + \frac{1}{\alpha^2}\right)}$$

Fig. 4 shows the relationship between k_s and α where $\alpha < 0.8$. In the same way as the problem of a floating ice plate (Kerr, 1976), the k_s can be very closely approximated by the linear function of α between 0.15 and 0.35. Eq.(10) shows the straight line connecting ($\alpha=0.2$, $k_s=0.8467$) and ($\alpha=0.3$, $k_s=1.0683$) where $v=0.3$. Using Eq.(10), structural safety when human weight of 100 kg is loaded on the ice dome is numerically examined as follows:

$$k_{sA} = 0.4035(1 + 5.492\alpha) \quad (10)$$

Assuming that the shoe size is 10cm \times 30cm, the equivalent radius a is estimated at 10 cm for the same area.

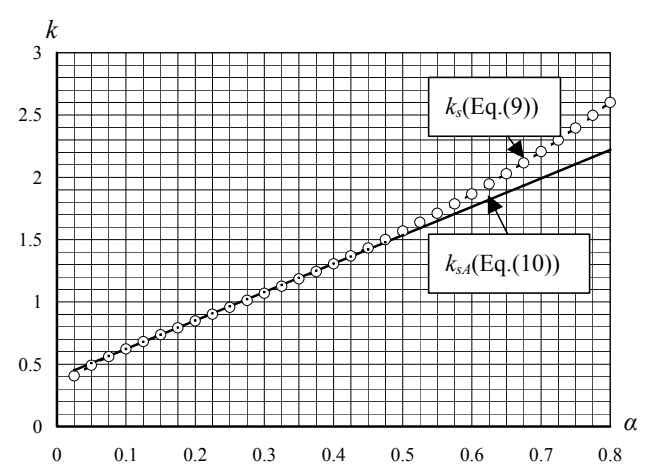


Fig.4 Comparison between k_s (Eq. (9)) and k_{sA} (Eq. (10))

$$\text{Using } v=0.3, \alpha = \frac{a}{l} = \frac{a}{\sqrt{Rh}} \sqrt[4]{12(1-v^2)} = \frac{18.18}{\sqrt{Rh}}$$

Furthermore, assuming that the open angle of the dome is 120° , the final expression of α becomes $\alpha = \frac{23.93}{\sqrt{D_s h}}$, where D_s is the diameter of the dome at the base.

Table 1 shows the numerical results where $D_s=15$ m and 30 m.

Table 1 Numerical result of single load ($P_t=100$ kg)

D_s (m)	h (cm)	α	k_{sA}	σ_{max} (kg/cm ²)
15	5	0.276	1.016	3.94
	6	0.252	0.962	2.89
30	6	0.178	0.799	3.48
	7	0.165	0.769	2.65

Here, the compressive membrane stress σ_c (kg/cm²) is computed 0.37 kg/cm² for $D_s=15$ m and 0.74 kg/cm² for $D_s=30$ m based on the membrane theory in shell under the gravity load and these σ_c are neglected in the Table 1 for the safety side of the evaluation. According to an experiment of ice beams (see APPENDIX-2), the short-term flexural strength of the ice is assumed to be 10 kg/cm². Because good quality of ice is produced artificially by the careful application of snow by blowing and water by spraying onto a pneumatic membrane, the density of the ice becomes about 0.85 g/cm³ polycrystalline ice. If the allowable stress is evaluated at 3.0 kg/cm² and σ_{max} does not exceed 3 kg/cm², it is judged that the dome is thick enough to have structural

safety against a short-term bending failure. As a result, the minimum thickness of the ice is 6 cm for spans up to 15 m, and 7 cm for spans between 15 m and 30 m at the base.

Twin Loads

The problem where the ice dome is subjected to the same size and weight of two circular uniform loads keeping the distance, s , between the central points, is discussed here. As seen in the results in previous section, the tensile stress on the inner surface of the shell under single loading has the following relationship $\sigma_t \geq \sigma_r$, where σ_t and σ_r are circumferential and radial bending stress, respectively, and the both are equal directly below the centre point of the load. The σ_s or $f_s(x)$, is given by the following Eq.(11).

$$\sigma_s = \frac{M_t}{\left(\frac{h^2}{6}\right)} + \frac{N_t}{h} = f_s(x) \left(\frac{P_t}{h^2}\right),$$

$$f_s(x) = \begin{cases} = -\left(\frac{6}{\pi}\right) \left[\frac{(\ker \alpha)}{\alpha} \left\{ -\nu beix + (1-\nu) \frac{ber' x}{x} \right\} - \left(\frac{kei \alpha}{\alpha}\right) \left\{ \nu berx + (1-\nu) \frac{bei' x}{x} \right\} \right] \\ - \left(\frac{\sqrt{12(1-\nu^2)}}{\pi}\right) \left\{ \left(\frac{kei' \alpha}{\alpha}\right) \left(-beix - \frac{ber' x}{x}\right) + \left(\frac{ker' \alpha}{\alpha}\right) \left(berx - \frac{bei' x}{x}\right) + \frac{1}{2\alpha^2} \right\}, & 0 \leq x \leq \alpha \\ = -\left(\frac{6}{\pi}\right) \left[\frac{ber' \alpha}{\alpha} \left\{ -\nu keix + (1-\nu) \frac{ker' x}{x} \right\} - \left(\frac{bei' \alpha}{\alpha}\right) \left\{ \nu kerx + (1-\nu) \frac{kei' x}{x} \right\} \right] \\ - \left(\frac{\sqrt{12(1-\nu^2)}}{\pi}\right) \left\{ \left(\frac{bei' \alpha}{\alpha}\right) \left(-keix - \frac{ker' x}{x}\right) + \left(\frac{ber' \alpha}{\alpha}\right) \left(kerx - \frac{kei' x}{x}\right) - \frac{1}{2x^2} \right\}, & x \geq \alpha \end{cases} \quad (11)$$

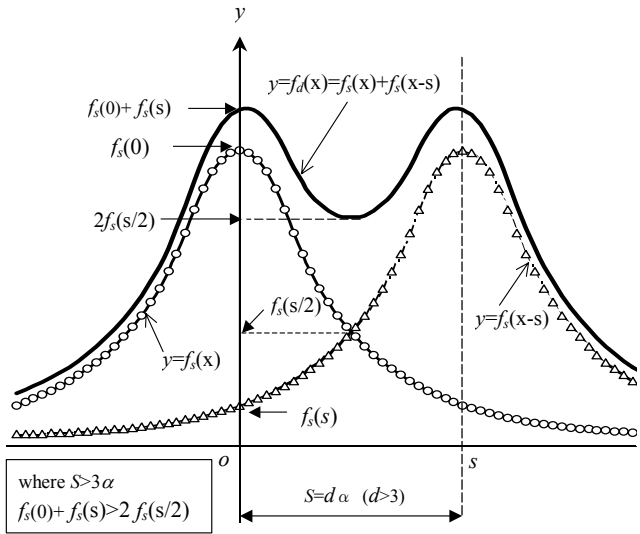


Fig.5 Stress distribution under twin loads

Fig.5 shows two curves of f_s : one $f_s(x)$ and the other $f_s(x-s)$. The aim of the subject here is to find out the exact maximum value of $f_d(x)(=f_s(x)+f_s(x-s))$ where $0 \leq x \leq s/2$. However, comparing the values of both ends, $f_d(0)(=f_s(0) + f_s(s))$ and $f_d(\frac{s}{2})(=2f_s(\frac{s}{2}))$, the larger one is considered the maximum value f_{dmax} in the twin loading problem. As s is clearly larger than 2α , therefore, the following Eqs.(12.a-c) are given according to the range of s .

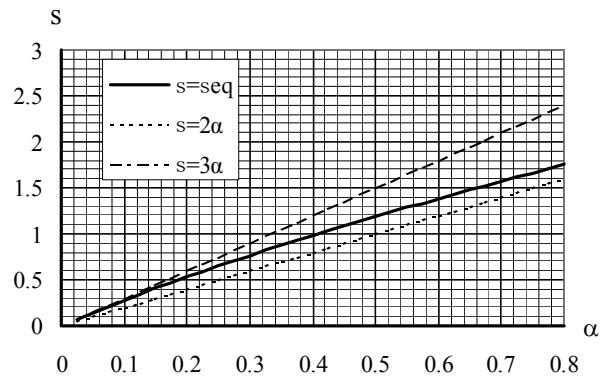


Fig.6 S - α Curve

$$\text{where } 2\alpha < s < s_{eq}, \quad f_d\left(\frac{s}{2}\right) > f_d(0) \quad (12.a)$$

$$\text{where } s = s_{eq}, \quad f_d\left(\frac{s}{2}\right) = f_d(0) \quad (12.b)$$

$$\text{where } s > s_{eq}, \quad f_d\left(\frac{s}{2}\right) < f_d(0) \quad (12.c)$$

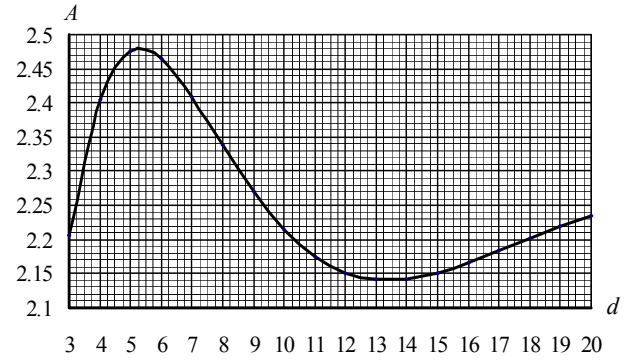


Fig.7a A - α curve

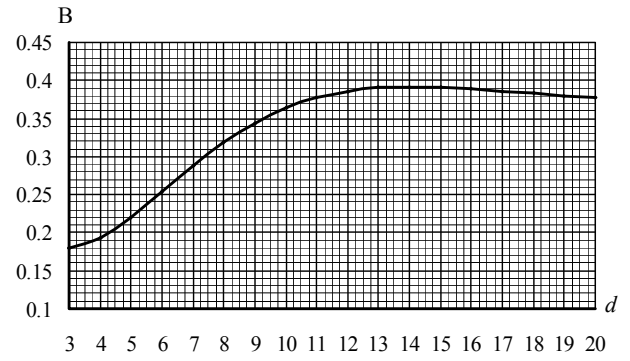


Fig.7b B - α curve

In solving Eq.(12.b), the s_{eq} - α curve is found in the region between $s=2\alpha$ and $s=3\alpha$. Therefore, where $s = d\alpha$ ($d \geq 3$), $f_d\left(\frac{s}{2}\right) < f_d(0)$ is found. $f_d(0)$ is given through Eq.(13).

Table 2 Numerical result of twin loads ($P_t=100$ kg)

D_s (m)	h (cm)	α	d	$A(d)$	$B(d)$	k_{da}	$\sigma_{dmax}(\text{kg}/\text{cm}^2)$
15	6	0.252	5	2.4766	0.22036	0.844	3.29
			10	2.2153	0.36382	0.922	3.01
30	7	0.165	5	2.4766	0.22036	0.629	3.24
			10	2.2153	0.36382	0.729	2.80

$$f_d(0) = -\left(\frac{6}{\pi}\right)\left[\frac{ber'\alpha}{\alpha}\{-\nu kei(d\alpha) + (1-\nu)\frac{ker'(d\alpha)}{(d\alpha)}\} - \frac{bei'\alpha}{\alpha}\{\nu ker(d\alpha) + (1-\nu)\frac{kei'(d\alpha)}{(d\alpha)}\}\right] - \frac{\sqrt{12(1-\nu^2)}}{\pi}\left\{\frac{bei'\alpha}{\alpha}\left(-kei(d\alpha) - \frac{ker'(d\alpha)}{(d\alpha)}\right) + \frac{ber'\alpha}{\alpha}\left(kei(d\alpha) - \frac{kei'(d\alpha)}{(d\alpha)}\right) - \frac{1}{2(d\alpha)^2}\right\} + \left(\frac{3}{\pi}\right)(1+\nu)\left(\frac{kei'\alpha}{\alpha}\right) - \frac{\sqrt{12(1-\nu^2)}}{2\pi}\left(\frac{ker'\alpha}{\alpha} + \frac{1}{\alpha^2}\right) \quad \dots \quad (13)$$

In accordance with the previous single loading problem, the loading coefficient $k_d = \frac{1}{f_d(0)}$ is approximated through a linear equation of α as shown in Eq.(14)

$$k_{da} = A(d)\alpha + B(d) \quad (14)$$

$A(d)$ and $B(d)$ of Eq.(14) are shown in Fig.7a and Fig.7b, respectively, and $\lim_{d \rightarrow \infty} A(d)$ and $\lim_{d \rightarrow \infty} B(d)$ are 2.2160 and 0.4035, respectively which agree with the coefficients of Eq.(10).

Based on the approximate curve in Fig.(7a,b) and Eq.(14), a numerical result is presented in Table 2.

As seen in the table, it is concluded that the minimum thickness for the ice is 6 cm for spans up to 15 m, and 7 cm for spans between 15 m and 30 m. It is also true for twin loads when the loading distance is 1 m apart.

CONCLUDING REMARKS

This paper described a numerical investigation of structural safety when the ice dome is subjected to a concentrated load a human live load on the apex. Regarding the problem as a short-term loading and the elastic behavior of ice, the elastic solution is based on the theory of a spherical shallow shell under a uniformly small circular load. Both the cases of single load and twin loads on a dome are investigated, assuming that the ice dome will break when the tensile stress reaches a certain maximum value. Estimating that the weight of a human is 100 kg and the allowable stress of the ice is 3 kg/cm², where the flexural strength is 10 kg/cm², it is concluded that the minimum thickness of the ice becomes 6 cm under a 15 m span, and 7 cm over a 15 m up to 30 m span, even though the distance is 1 m in case of twin loads. On the other side, according to the previous experiments of the reduced models of ice dome under a short-term circular load on the apex, the ultimate failure loads were found to be higher than the first cracking load (Kokawa and Hirasawa, 1982/1983). Therefore, it seems that the minimum thickness given in this paper is thick enough to have structural safety against the short-term failure.

As the ice thickness of the completed ice dome is normally in the range of 12 to 25 cm corresponding to the ice dome's span ranging from 10 to 30 m, it is clear that an adequate level of safety will be achieved for the subject being addressed because the above-mentioned minimum thickness is greatly exceeded. However, as the ice plate during a construction work and a removal snow for the maintenance, might be thinner than the completion, the proposed simplified formula will be useful for checking the structural safety.

This paper assumed 3 kg/cm² as the allowable flexural stress in the ice, considering that the ice in the dome has a good quality to build up by a careful application of blowing snow and spraying water onto a formwork and it can be expected the flexural strength of the ice exceeds 10 kg/cm² (see Appendix-2).

In order to evaluate the minimum thickness of an ice dome in detail more, the following two subjects must be investigated in the future.

(1) The short-term flexural strength of the ice produced by blowing snow and spraying water.

(2) The initial cracking load and the ultimate failure load of an ice dome under a concentrated circular load on the apex.

APPENDIX-1: INDUCEMENT OF ELASTIC SOLUTION

The fundamental solutions w_f, F_f under a concentrated load P are given by Eq.(A-1) (Timoshenko, S. P. and Woinoesky-Krieger, S., 1959a).

$$w_f = -\frac{\sqrt{3(1-\nu^2)}}{\pi} \frac{PR}{Eh^2} keix \quad F_f = -\frac{PR}{2\pi} (\ker x + \log x) \quad \left. \right\} \quad (A-1)$$

$$\text{Where } x = \frac{r}{l}, \quad l = \left(\frac{Rh}{\sqrt{12(1-\nu^2)}} \right)^{\frac{1}{2}}, \quad l: \text{characteristic length}$$

And, w_f is the solution for vertical displacement in an elastic plate under a concentrated load, which is expressed in the same way as the solution for Hertz's problem (Timoshenko, S. P. and Woinoesky-Krieger, S., 1959b). Therefore, the solution for w under the circular uniform load in this problem is given in Eqs. (2) and (3) of this paper by replacing the characteristic length in Wyman's solution (Wayman, 1950) with that of Eq.(A-1).

The solution of stress function, F , is induced by first finding the solution under a ring load, F_r . Referring to Fig.A-1, dF_r at point Q is

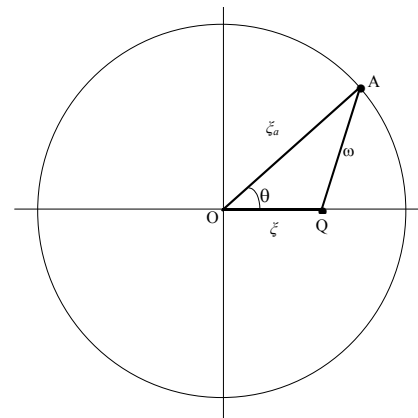


Fig. A-1 Addition theorem

written in the following equation where point A is subjected to a concentrated load, $P (= q_i \xi_a l d\theta)$.

$$dF_r = -\frac{q_i \xi_a l R}{2\pi} (\ker \omega + \log \omega) d\theta$$

$$\omega = \sqrt{\xi_a^2 + \xi^2 - 2\xi_a \xi \cos \theta}$$

Where q_i is a constant load per unit length on the circle. Therefore, F_r at point Q is expressed by the following equation.

$$F_r = \int dF_r = -\frac{q_i \xi_a l R}{\pi} \int_0^\pi (\ker \omega + \log \omega) d\theta$$

where $\int_0^\pi \ker \omega d\theta$ is expressed in Eq.(A-2) using Addition Theorem of $\ker \omega$ (Watson, 1922).

$$\int_0^\pi \ker \omega d\theta = \begin{cases} \pi(\ker \xi_a \text{ber} \xi - \text{kei} \xi_a \text{bei} \xi), & \xi \leq \xi_a \\ \pi(\ker \xi \text{ber} \xi_a - \text{kei} \xi \text{bei} \xi_a), & \xi \geq \xi_a \end{cases} \quad (\text{A-2})$$

$\int_0^\pi \log \omega d\theta$ is expressed in Eq.(A-3) (Moriguchi *et al.*, 1971).

$$\int_0^\pi \log \omega d\theta = \begin{cases} \pi \log \xi_a, & \xi \leq \xi_a \\ \pi \log \xi, & \xi \geq \xi_a \end{cases} \quad (\text{A-3})$$

Finally, the solution for stress function under ring load, F_r is given by Eq.(A-4).

$$F_r = \begin{cases} -Rl q_i \xi_a \{(\ker \xi_a \text{ber} \xi - \text{kei} \xi_a \text{bei} \xi) + \log \xi_a\}, & \xi \leq \xi_a \\ -Rl q_i \xi_a \{(\text{ber} \xi_a \ker \xi - \text{bei} \xi_a \text{kei} \xi) + \log \xi\}, & \xi \geq \xi_a \end{cases} \quad (\text{A-4})$$

The solution, F , under circular uniform load is given by superimposing F_r to radial direction: $q = qdr = qld\xi$, where q is a constant load per unit area.

$$dF_{ri} = -Rl^2 q \xi \{(\ker \xi \text{ber} x - \text{kei} \xi \text{bei} x) + \log x\} d\xi, \quad x \leq \xi$$

$$dF_{ro} = -Rl^2 q \xi \{(\text{ber} \xi \ker x - \text{bei} \xi \text{kei} x) + \log x\} d\xi, \quad x \geq \xi$$

$$F = \begin{cases} \int_{\xi=x}^{\xi_a} dF_{ri} + \int_0^{\xi=x} dF_{ro}, & 0 \leq x \leq \xi_a \\ \int_0^{\xi_a} dF_{ro}, & x \geq \xi_a \end{cases} \quad (\text{A-5})$$

Executing the integration of the right side in Eq.(A-5), Eqs.(2) and (3) in this paper can be obtained.

APPENDIX-2: FLEXURAL STRENGTH OF ICE BEAM

The ice of the shell belongs to T1 snow ice considered to be isotropic (Michel, 1978). Tensile strength of polycrystalline ice is relatively strain rate ($10^0 \sim 10^{-6}$ /sec) and temperature independent (Mellor, 1979). The flexural strength is also independent from strain rate, temperature (Sinha *et al.*, 1987) and stress rate ($0.1 \sim 10$ kg/cm²/sec) (Hirayama *et al.*, 1990). Therefore, a short-term bending experiment with a loading-period of less than 10 seconds was conducted in order to test the flexural strength of an ice beam without careful controlled strain rate and stress rate. As in the construction of ice shells, these ice beams were made by freezing a mixture of snow and water outdoors in natural sub-freezing temperatures. The approximate dimensions were 50 cm in length (L), 8 cm in width (b) and 4 cm in thickness (h).

The bending strength σ_f of the simply supported, centre-loaded ice beams was computed according to the relationship:

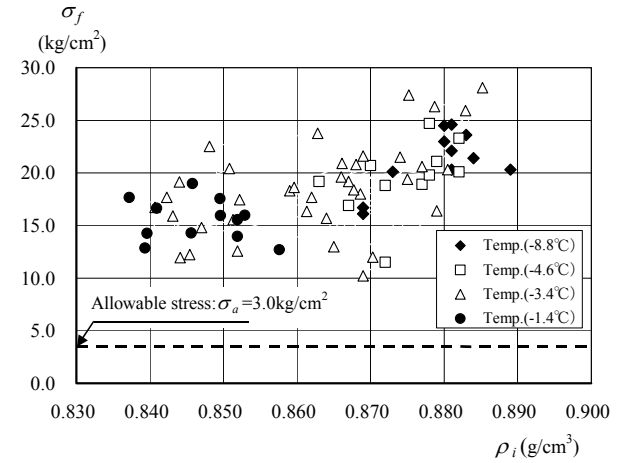


Fig. A-2 Flexural strength of simply supported ice beam

$$\sigma_f = \frac{3PL}{2bh^2}$$

Where P is the force at failure. P was electrically measured with a 100 kg capacity load cell. Fig. A-2 shows the relationship between σ_f and ρ_i , the density of the ice. Based on the result, 10 kg/cm² was the smallest value in this experiment.

REFERENCES

Hirayama, K., Ishida, H., Sakai, S., Sakamoto, M., Maeda, T. and Ahashi, N., (1990). "Parametric Expressions for ice Compressive and Flexural Strength," *Proc. of IAHR Ice Symposium*, Espoo, 196-209.

Kerr, A.D., (1976). "The Bearing Capacity of Floating Ice Plates Subjected to Static or Quasi-Static Loads," *J. Glaciology*, 17, 229-268.

Kokawa, T. and Hirasawa, I., (1982/1983). "On the Behavior of Ice Domes under Short-term Loading (in Japanese)," *Bull. Hokkaido Tokai Univ.*, Vol.3/4, 77-85.

Kokawa, T., (1985). "Experimental Studies on Ice Shell in Asahikawa," *Cold Regions Science and Technology*, Vol. 11, 150-170.

Kokawa, T. and Murakami, K., (1986). "Challenge to 20-m Span Ice Dome," Shells, Membrane and Space Frames, *Proceeding IASS Symposium Osaka*, Vol.1, 297-304.

Kokawa, T., (1988). "Construction and Creep Test of 15-m Span Ice Dome," *Proceeding of IAHR Ice Symposium Sapporo*, 390-399.

Kokawa, T., Watanabe, K. and Itoh, O., (2000). "Ice Shell—Recent Application to Winter Architecture," *Proc. 10th Int. Offshore and Polar Eng. Conf.*, Seattle, ISOPE, Vol. 1, 716-721.

Kokawa, T., (2002). "Field Experiment of Ice Dome Spanning 20~30 Meters," *Int. Journal of Offshore and Polar Engineering*. Vol. 12, No. 4, 264-270.

Mellor, M., (1979). "Mechanical Properties of Polycrystalline Ice," *IUTAM Symposium Copenhagen 1979, Physics and Mechanics of Ice*, 217-245.

Michel, B., (1978). "Ice mechanics," Les Presses de l'Universite Laval, Quebec Canada.

Moriguchi, S., Udagawa, K., Ichimatsu, S., (1971). "Formula of Mathematics III (in Japanese)," pp. 174-177., Iwanami Zenshyo.

Sinha, N.K., Timco, G.W. and Frederking, R., (1987). "Recent advances in ice mechanics in Canada," *Appl. Mech. Rev.* Vol. 40, no. 9, Sep. 1987, 1214-1231.

Timoshenko, S. P. and Woinoensky-Krieger, S., (1959a). "Theory of Plates and Shells," McGraw-Hill, London, 2nd Ed., 558-561.

Timoshenko, S. P. and Woinoensky-Krieger, S., (1959b). "Theory of Plates and Shells," McGraw-Hill, London, 2nd Ed., 259-269.

Watson, G.N., (1922). "Treatise on the Theory of Bessel Functions," 358-372., Cambridge.

Wyman, M., (1950). "Deflection of an Infinite Plate," *Canadian Journal of Research*, Ser. A, Vol. 28, 293-302.